

Contribution from the Department of Chemistry, Swedish University of Agricultural Sciences, P.O. Box 7015, S-750 07 Uppsala, Sweden, Department of Inorganic Chemistry, The Royal Institute of Technology, S-100 44 Stockholm, Sweden, and Daresbury Laboratory, Daresbury, Warrington WA4 4AD, United Kingdom

A Large-Angle X-ray Scattering, XAFS, and Vibrational Spectroscopic Study of Copper(I) Halide Complexes in Dimethyl Sulfoxide, Acetonitrile, Pyridine, and Aqueous Solutions

Ingmar Persson,^{*,†} Magnus Sandström,^{*,‡} Andrew T. Steel,[§] Maria J. Zapatero,^{‡,||} and Ralf Åkesson[‡]

Received March 22, 1991

The structures of some halocuprate(I) complexes in acetonitrile, dimethyl sulfoxide, pyridine, and aqueous solutions and the solvated copper(I) bromide complex in pyridine and acetonitrile solutions have been studied by EXAFS (extended X-ray absorption fine structure) and vibrational spectroscopic techniques. The LAXS (large-angle X-ray scattering) method has been applied for structural characterization of concentrated bromo- and iodocuprate(I) solutions in dimethyl sulfoxide and acetonitrile. The linearity of the dihalocuprate(I) complexes CuX_2^- ($\text{X} = \text{Cl}, \text{Br}, \text{I}$) is found to be retained in the nonaqueous solvents studied. From EXAFS measurements Cu-Cl and Cu-Br distances of 2.11 (2) and 2.22 (2) Å, respectively, are obtained with no coordination of solvent molecules to the copper(I) ion. The tendency of the dihalocuprate(I) complexes to dimerize increases with increasing concentration and size of the halide ligand. The equilibrium constants for the dimerization reaction $2\text{CuX}_2^- \rightleftharpoons \text{Cu}_2\text{X}_4^{2-}$ are estimated to be <0.2 , ≈ 2 , and $>100 \text{ mol}^{-1} \text{ dm}^3$ for concentrated chloro-, bromo-, and iodocuprate(I) solutions in dimethyl sulfoxide, respectively. The coordination around copper(I) in the dimers is found to be trigonal with one terminal and two bridging halide atoms. The average Cu-X bond distances obtained by the LAXS method, are 2.38 (1) and 2.58 (1) Å for the $\text{Cu}_2\text{Br}_4^{2-}$ and $\text{Cu}_2\text{I}_4^{2-}$ complexes, respectively. The EXAFS data are consistent with a Cu-Cl distance of 2.21 (3) Å for a trigonal trichlorocuprate(I) complex in aqueous solution and with a tetrahedral $[\text{CuBr}(\text{py})_3]$ structure with one Cu-Br and three Cu-N distances of 2.41 (3) and 2.06 (3) Å, respectively, for copper(I) bromide in pyridine solution. The shapes of the X-ray absorption edges are markedly different for copper(I) in linear and trigonal coordinations and have been used to obtain information on the coordination geometry around copper(I) for the halocuprate(I) complexes in this study. Raman and far-IR spectra have been measured for the CuX_2^- , $\text{Cu}_2\text{Br}_4^{2-}$, and $\text{Cu}_2\text{I}_4^{2-}$ ions in solids and solution, with only minor shifts in the vibrational frequencies in solution indicating small perturbations of the structure and weak solvation effects. The Cu-N stretching vibration frequencies have been measured for the solid $[\text{Cu}(\text{py})_4]\text{ClO}_4$ compound.

Introduction

The complex formation of copper(I) in solution with the halide ions, $\text{X} = \text{Cl}, \text{Br}, \text{and I}$, has been studied by thermodynamic methods in a number of solvents including water,¹⁻³ acetonitrile,^{1,4} dimethyl sulfoxide,^{1,5} and pyridine.^{1,6,7} Monomeric CuX and CuX_2^- complexes have been found to be present in the aprotic solvents studied.^{1-6,8} A third mononuclear complex CuX_3^{2-} has been reported in aqueous solution,^{2,3} and in dimethyl sulfoxide as a very weak chloride complex.⁵ Polynuclear halocuprate(I) complexes have been proposed in aqueous solution from solubility measurements,²⁻⁴ and dinuclear iodide complexes have been postulated in dimethyl sulfoxide.⁵

Jagner et al. have made an extensive crystallographic study of halocuprate(I) complexes, in which the size of the cation has been varied systematically.⁹⁻¹¹ The tendency to form mononuclear halocuprate(I) complexes was found to increase with increasing size of the cation. However, if dihalocuprate(I) compounds with the same cation are compared, an increasing tendency to dimerization is found in the order $\text{Cl} < \text{Br} < \text{I}$, i.e. with increasing size of the halide. Thus, it has only been possible to isolate mononuclear CuI_2^- complexes in the solid state by using potassium crown ether complexes as cations, owing to the large tendency of the iodocuprate(I) complexes to polymerize. Linear diiodocuprate(I) ions have been found in the compounds $[\text{K}(18\text{-crown-6})]\text{CuI}_2$ and $[\text{K}(\text{dicyclohexano-18-crown-6})]\text{CuI}_2$ with Cu-I distances of 2.383 (1) and 2.394 (2) Å, respectively.¹²

Bowmaker and co-workers have made structural and spectroscopic characterizations of several mononuclear and polymeric halocuprate(I) complexes¹³⁻¹⁶ and discussed bonding theories for linear complexes of d^{10} ions in an extensive review article.¹⁷ The structures of a number of iodocuprates(I) have been determined by Hartl and co-workers.¹⁸⁻²⁰

The coordination geometry around the copper atom in the halocuprate(I) compounds has been reported to be essentially linear, trigonal, or tetrahedral in the large number of monomeric

- (1) (a) Sillén, L. G.; Martell, A. E., Eds. *Stability Constants of Metal-Ion Complexes*; Special Publication Nos. 17 and 25; Chemical Society: London, 1965 and 1971. (b) Högföldt, E., Ed. *Stability Constants of Metal-Ion Complexes*; IUPAC Chemical Data Series No. 21; Pergamon: Oxford, England, 1982; Part A.
- (2) (a) Ahrland, S.; Rawsthorne, J. *Acta Chem. Scand.* **1970**, *24*, 157. (b) Ahrland, S.; Tagesson, B. *Acta Chem. Scand., Ser. A* **1977**, *31*, 615.
- (3) (a) Fritz, J. J. *J. Phys. Chem.* **1981**, *85*, 890. (b) Fritz, J. J. *J. Phys. Chem.* **1984**, *88*, 4358. (c) Fritz, J. J.; Luzik, E. *J. Solution Chem.* **1987**, *16*, 79.
- (4) Ahrland, S.; Nilsson, K.; Tagesson, B. *Acta Chem. Scand., Ser. A* **1983**, *37*, 193.
- (5) Ahrland, S.; Bläuenstein, P.; Tagesson, B.; Tuhtar, D. *Acta Chem. Scand., Ser. A* **1980**, *34*, 265.
- (6) Ahrland, S.; Ishiguro, S.-I.; Persson, I. *Acta Chem. Scand., Ser. A* **1986**, *40*, 418.
- (7) The abbreviations Me₂SO = dimethyl sulfoxide; MeCN = acetonitrile, and py = pyridine will be used.
- (8) Johnsson, M.; Persson, I.; Portanova, R. *Inorg. Chim. Acta* **1987**, *127*, 35.
- (9) (a) Andersson, S.; Jagner, S. *Acta Chem. Scand., Ser. A* **1986**, *40*, 52. (b) Andersson, S.; Jagner, S. *Acta Chem. Scand., Ser. A* **1986**, *40*, 177. (c) Andersson, S.; Jagner, S. *Acta Chem. Scand., Ser. A* **1987**, *41*, 230. (d) Andersson, S.; Jagner, S. *Acta Chem. Scand., Ser. A* **1988**, *42*, 681. (e) Andersson, S.; Jagner, S. *Acta Chem. Scand., Ser. A* **1989**, *43*, 39 and references therein.
- (10) Andersson, S.; Håkansson, M.; Jagner, S. *J. Crystallogr. Spectrosc. Res.* **1989**, *19*, 147 and references therein.
- (11) Andersson, S. On the Formation and Structure of Halocuprate(I) Ions in the Solid State. Ph.D. Thesis, University of Gothenburg, 1988.
- (12) (a) Rath, N. P.; Holt, E. *J. Chem. Soc., Chem. Commun.* **1986**, 311. (b) Holt, E. Personal communication.
- (13) Bowmaker, G. A.; Brockliss, L. D.; Whiting, R. *Aust. J. Chem.* **1973**, *26*, 29.
- (14) Bowmaker, G. A.; Brockliss, L. D.; Earp, C. D.; Whiting, R. *Aust. J. Chem.* **1973**, *26*, 2593.
- (15) Bowmaker, G. A.; Clark, G. R.; Rogers, D. A.; Camus, A.; Marsich, N. *J. Chem. Soc., Dalton Trans.* **1984**, 37.
- (16) Bowmaker, G. A.; Camus, A.; Skelton, B. W.; White, A. H. *J. Chem. Soc., Dalton Trans.* **1990**, 727.
- (17) Bowmaker, G. A. *Adv. Spectrosc.* **1987**, *14*, 1.
- (18) (a) Hartl, H.; Brüdgam, I.; Mahdjour-Hassan-Abadi, F. *Z. Naturforsch.* **1983**, *38B*, 57. (b) Hartl, H.; Brüdgam, I.; Mahdjour-Hassan-Abadi, F. *Z. Naturforsch.* **1985**, *40B*, 1032.
- (19) Hartl, H. *Angew. Chem.* **1987**, *99*, 925.
- (20) Bigalke, K. P.; Hans, A.; Hartl, H. *Z. Anorg. Allg. Chem.* **1988**, *563*, 96.

[†] Swedish University of Agricultural Sciences.

[‡] The Royal Institute of Technology.

[§] Daresbury Laboratory. Present address: Unilever Research, Port Sunlight Laboratory, Quarry Rd. East, Bebington, Wirral, Merseyside L63 3JW, U.K.

^{||} Present address: Department of Chemistry, University of Pais Vasco, Apartado 644, E-48080 Bilbao, Spain.

Table I. Compositions of the Solutions in mol dm⁻³

solution	Cu ⁺	X ⁻	NH ₄ ⁺	Li ⁺	Na ⁺	Et ₄ N ⁺	solvent
0.5 M Cu/Cl(MeCN) ^a	0.500	1.500				1.000	19.1
1 M Cu/Cl(Me ₂ SO)	1.02	3.02		2.00			12.4
0.1 M Cu/Cl(py)	0.109	0.61		0.50			12.3
0.2 M Cu/Cl(H ₂ O)	0.220	8.75		8.53			55
88 mM Cu/Br(MeCN)	0.088	0.159				0.071	19.0
1.5 M Cu/Br(Me ₂ SO)	1.50	3.75	2.25				11.9
0.4 M CuBr(py)	0.393	0.393					12.0
50 mM Cu/I(MeCN)	0.050	0.151			0.101		19.1
1 M Cu/I(MeCN)	1.00	2.00			1.00		17.7
1.5 M Cu/I(Me ₂ SO)	1.50	3.72	2.22				12.6

^a Diluted 10 times before the EXAFS investigation and then denoted 50 mM Cu/Cl(MeCN).

or bridged compounds studied. However, no monomeric CuX₄³⁻ complexes have been found in crystal structures,^{17,19,21} although stability constants are reported for weak CuCl₄³⁻ and CuI₄³⁻ complexes in aqueous solution.^{1,2}

A large number of crystal structures of adducts (1:1) between nitrogen donor solvent molecules and copper(I) halides, which in some cases also contain discrete halocuprate(I) anions without additional ligands, have been determined mainly by Healy, White, and co-workers.²¹⁻³⁰ The prevailing structural features are cubane or "stair" halide-bridged polymers in which the copper(I) ions have a tetrahedral surrounding, trigonal dimers, and linear monomers.

Vibrational spectroscopy provides a convenient way to distinguish a linear (*D_{∞h}*) from a bent (*C_{2v}*) structure of an AB₂ species, as the selection rules for a centrosymmetric species exclude any coincidences between IR and Raman spectra. Waters and Basak have made a vibrational spectroscopic study of CuX₂⁻ ions (X = Cl, Br, I) in tri-*n*-butyl phosphate solution and concluded that all three ions do obey *D_{∞h}* symmetry rules.³¹ Raman and IR vibrational spectra of the linear CuCl₂⁻ and CuBr₂⁻ complexes in the solid state, and also of Cu₂Br₄²⁻ and Cu₂I₄²⁻, have been reported previously.^{13,17}

The purpose of this study is to determine the structures of halocuprate(I) complexes formed in solvents of different coordinating properties. Distances from a central copper(I) to ligand atoms have been obtained by means of EXAFS (extended X-ray

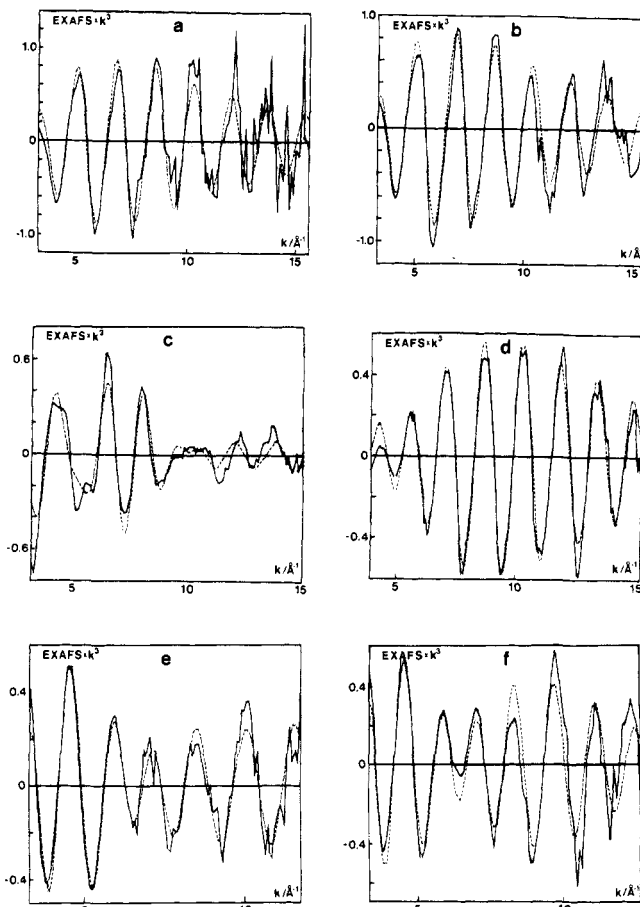


Figure 1. Curve-fitting of weighted unfiltered EXAFS data ($k^2\chi$) of some of the solutions studied with parameters according to Table II: (a) 50 mM Cu/Cl(MeCN); (b) 1 M Cu/Cl(Me₂SO); (c) 0.4 M Cu/Br(py); (d) 1.5 M Cu/Br(Me₂SO); (e) 1.5 M Cu/I(Me₂SO); (f) 1 M Cu/I(MeCN). The scattering variable k is equivalent to s in LAXS.

absorption fine structure) spectroscopy, the only technique which can be used to obtain bond distances for dilute solutions. The LAXS (large-angle X-ray scattering) method was used for three of the most concentrated solutions, since it allows not only Cu-X distances but also the intramolecular halide-halide interactions to be studied. A point of special interest is to determine whether the copper(I) ion in the dihalocuprate(I) complexes is solvated in its inner coordination sphere in a similar way as mercury(II) is in the HgX₂ complexes in solution.^{32,33} Vibrational spectroscopy provides a sensitive probe for solvent effects on the complexes, and Raman and IR spectra have been recorded for solutions of sufficiently high concentration.

Experimental Section

Preparation of Solids and Solutions. Copper(I) chloride, bromide, and iodide were prepared under nitrogen atmosphere according to standard methods,³⁴ and the tetrabutylammonium salts of the halocuprate(I) complexes as previously described.³⁵ The synthesis of [Cu(py)₄]ClO₄ is described elsewhere.³⁶ The compound [K(18-crown-6)]CuI₂ was obtained by adding a saturated aqueous solution of CuI in a large excess

- (21) Hathaway, B. J. In *Comprehensive Coordination Chemistry*; Wilkinson, G., Gillard, R. D., McCleverty, J. A., Eds.; Pergamon: Oxford, England, 1987; Vol. 5, Chapter 53.3.
- (22) Dyason, J. C.; Engelhardt, L. M.; Pakawatchai, C.; Healy, P. C.; White, A. H. *Aust. J. Chem.* **1985**, *38*, 1243.
- (23) Canty, A. J.; Engelhardt, L. M.; Healy, P. C.; Kildea, J. D.; Minchin, N. J.; White, A. H. *Aust. J. Chem.* **1987**, *40*, 1881 and references therein.
- (24) (a) Healy, P. C.; Kildea, J. D.; White, A. H. *Aust. J. Chem.* **1989**, *42*, 137. (b) Healy, P. C.; Kildea, J. D.; White, A. H. *J. Chem. Soc., Dalton Trans.* **1988**, 1637 and references therein.
- (25) (a) Healy, P. C.; Kildea, J. D.; Skelton, B. W.; White, A. H. *Aust. J. Chem.* **1989**, *42*, 79. (b) Healy, P. C.; Kildea, J. D.; Skelton, B. W.; White, A. H. *Aust. J. Chem.* **1989**, *42*, 93. (c) Healy, P. C.; Kildea, J. D.; Skelton, B. W.; White, A. H. *Aust. J. Chem.* **1989**, *42*, 115 and references therein.
- (26) (a) Engelhardt, L. M.; Healy, P. C.; Kildea, J. D.; White, A. H. *Aust. J. Chem.* **1989**, *42*, 107. (b) Engelhardt, L. M.; Healy, P. C.; Kildea, J. D.; White, A. H. *Aust. J. Chem.* **1989**, *42*, 185.
- (27) Graham, A. J.; Healy, P. C.; Kildea, J. D.; White, A. H. *Aust. J. Chem.* **1989**, *42*, 177.
- (28) Healy, P. C.; Skelton, B. W.; White, A. H. *J. Chem. Soc., Dalton Trans.* **1989**, 971.
- (29) Campbell, J. A.; Raston, C. L.; White, A. H. *Aust. J. Chem.* **1977**, *30*, 1937.
- (30) Eitel, E.; Oelkrug, D.; Hiller, W.; Strähle, J. *Z. Naturforsch.* **1980**, *35B*, 1247.
- (31) Waters, D. N.; Basak, B. *J. Chem. Soc. A* **1971**, 2733.

- (32) Persson, I.; Sandström, M.; Goggin, P. L. *Inorg. Chim. Acta* **1987**, *129*, 183.
- (33) Sandström, M.; Persson, I.; Persson, P. *Acta Chem. Scand.* **1990**, *44*, 653.
- (34) (a) Keller, R. N.; Wycoff, H. D. In *Inorganic Synthesis*; Fernelius, W. C., Ed.; McGraw-Hill: New York and London, 1946; Vol. 8, p 1. (b) Kaufmann, G. B. In *Inorganic Synthesis*; Fernelius, W. C., Ed.; McGraw-Hill: New York and London, 1960; Vol. 6, p 3. (c) Kaufmann, G. B. In *Inorganic Synthesis*; Rochow, E. G., Ed.; McGraw-Hill: New York and London, 1967; Vol. 11, p 215.
- (35) Nilsson, M. *Acta Chem. Scand., Ser. B* **1982**, *36*, 125.
- (36) Persson, I.; Penner-Hahn, J. E.; Hodgson, K. O. *Inorg. Chem.*, submitted for publication.

of KI to an equivalent amount of 18-crown-6 in acetone solution and refluxing the mixture for 3 h.¹² Colorless diamond-shaped crystals were formed on evaporation.

The halocuprate(I) solutions (Table I) were prepared by dissolving weighed amounts of the halides of copper(I), lithium, sodium, ammonium, or tetraethylammonium in degassed solvents. The choice of cations was based mainly on solubility considerations, as this is a limiting factor for the LAXS and vibrational spectroscopy measurements. In order to prevent oxidation of copper(I) or iodide ions, the solutions were stored under nitrogen atmosphere and in contact with metallic copper.

EXAFS Measurements. Copper K-edge X-ray absorption data were collected in transmission mode at ambient temperature at the Synchrotron Radiation Source, SRS, Daresbury Laboratory, under dedicated conditions (2.0 GeV, maximum current 150 mA) using the wiggler station 9.2. A Si(220) double monochromator was used at 50% of maximum intensity in order to reduce higher order harmonics. The energy scale of all spectra was fixed by simultaneously recording the spectrum of a copper foil in all experiments, using the first inflection point of metallic copper at 8980.3 eV³⁷ for the calibration. The EXAFS data treatment was carried out by using the two different computer program packages XFPACK³⁸ and EXBACK + EXCURVE,³⁹ in order to estimate effects owing to the somewhat different procedures of preedge subtraction,⁴⁰ spline removal³⁸ or polynomial fitting,³⁹ and Fourier filtering.⁴⁰ In the curve-fitting procedures transferability of the phase shift and amplitude parameters between compounds of similar chemical structure of a specific element was assumed.⁴¹ EXAFS spectra of the solid compounds Cu₂O,⁴² [(C₄H₉)₄N]CuCl₂,⁴³ [(C₄H₉)₄N]CuBr₂,⁴³ and CuI⁴⁴ diluted with BN, and of a copper foil,⁴⁵ were recorded in order to obtain the interaction parameters for the Cu–O(N), Cu–Cl, Cu–Br, Cu–I, and Cu–Cu distances, respectively, which were used for evaluation of the corresponding distances to copper in the unknown structures. The solutions were kept in cells with thin Mylar windows and Teflon spacers (0.5–2 mm), which were placed in a nitrogen-filled box with Mylar windows during the measurements. For the dimethyl sulfoxide solutions, an IR cell with a 0.1-mm Teflon spacer and 1-mm polyethylene windows was used. The curve-fitting of some of the unfiltered EXAFS spectra is shown in Figure 1.

LAXS Measurements. A large-angle θ – θ diffractometer, described previously,⁴⁶ was used to measure the X-ray scattering (Mo K α radiation, $\lambda = 0.7107$ Å), from the surface of the solution contained in a glass cup under nitrogen atmosphere, enclosed in a Teflon cylinder with an X-ray window of polyethylene-coated Al foil. The scattered intensities were measured at 400 discrete points in the region $2 < \theta < 70^\circ$. The scattering angle is 2θ . At least 10^5 counts were accumulated at each point, which corresponds to a statistical error of about 0.3%. The data reduction was performed as described previously^{47,48} by means of the program KURVLR.⁴⁹ The scattering factors f for neutral atoms, corrections for anomalous dispersion, $\Delta f'$ and $\Delta f''$, and values for incoherent scattering were taken from the same sources as before.⁴⁸ The RDF's $D(r) - 4\pi r^2 \rho_0$, obtained by Fourier transformation of the experimental reduced intensity functions $i_{\text{exp}}(s)$, are shown in Figure 2. Theoretical intensity values for atomic pair interactions within the proposed molecular models of complexes and solvent molecules were calculated according to a Debye expression:^{48,49}

$$i_c(s) = \sum_{p \neq q} \sum [f_p(s) f_q(s) + \Delta f_p'' \Delta f_q''] (\sin sr_{pq}) (sr_{pq})^{-1} \exp(-1/2 l_{pq}^2 s^2) \quad (1)$$

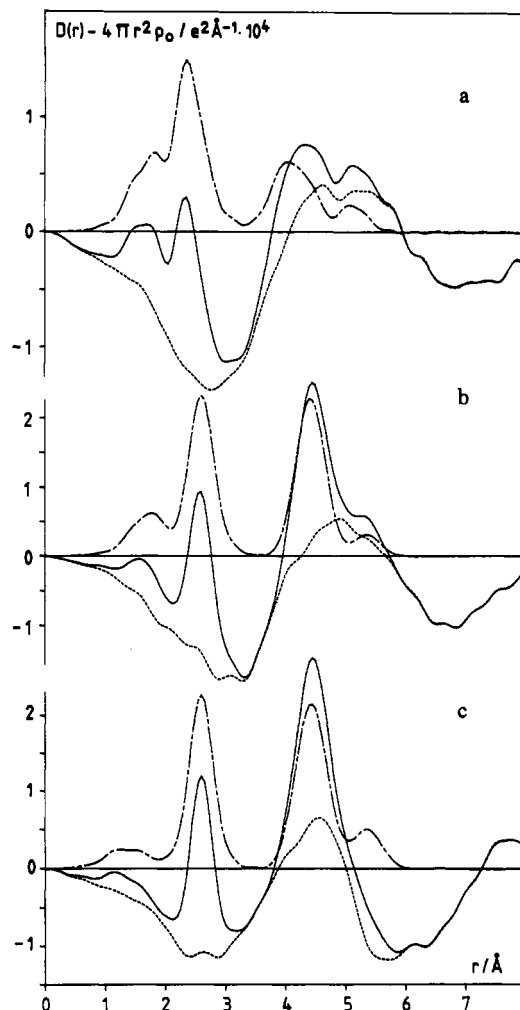


Figure 2. $D(r) - 4\pi r^2 \rho_0$ functions from LAXS studies and calculated peak shapes with parameters from Table III: (a) 1.5 M Cu/Br(Me₂SO); (b) 1.5 M Cu/I(Me₂SO); (c) 1 M Cu/I(MeCN). Experimental curves (solid lines), model functions (dot-dashed lines), and their differences (dashed lines) are shown.

where r_{pq} is the distance between the two atoms p and q in the pair and l_{pq} is the root-mean-square variation in the distance. Least-squares refinements on the intensity functions of the parameters of the proposed models were carried out by minimizing the expression $\sum s^2 [i_{\text{exp}}(s) - i_c(s)]^2$ with the use of the program STEPLR.⁵⁰ In the fitting range only high-angle data ($s > \sim 4 \text{ \AA}^{-1}$, with $s = 4\pi\lambda^{-1} \sin \theta$) for which the solvent-solvent and other long-range intermolecular interactions were found to be negligible,^{51,52} were included. Prior to the refinement, the $i_{\text{exp}}(s)$ function was corrected by removing spurious nonphysical peaks below 1.5 Å in the RDF's, which could not be related to intramolecular distances, by a Fourier back-transformation procedure.^{49,51}

Vibrational Spectroscopy. Far-infrared spectra were recorded with Nicolet 7199A and Perkin-Elmer 1700 FT-IR spectrometers at 4-cm⁻¹ resolution using Mylar beam splitters (effective spectral range 100–500 cm⁻¹), Globar sources, polyethylene-windowed DTGS detectors, and IR cells with polyethylene or silicon windows.

Raman spectra were excited with a Coherent Radiation Laboratories Innova 90-5 argon ion laser at 514.5 nm or 90-K krypton ion laser at 647.1 nm, with an effective power of usually less than 500 mW at the sample to avoid heating effects. Spectra were recorded with a DILOR Z24 triple monochromator using dc amplification or photon counting with spectral bandwidths of 4 cm⁻¹ for solutions and 2 cm⁻¹ for solids. Interfering bands were removed by spectral subtractions when necessary; in particular, care was taken to minimize interference with the strong Raman band at ca. 113 cm⁻¹ from triiodide ions,⁵³ which are easily

(37) Kau, L.-S.; Spira-Solomon, D. J.; Penner-Hahn, J. E.; Hodgson, K.; Solomon, E. I. *J. Am. Chem. Soc.* **1987**, *109*, 6433.

(38) Scott, R. A. *Methods Enzymol.* **1985**, *117*, 414.

(39) Pantos, E.; Firth, D. *EXAFS and Near Edge Structure*; Springer Verlag: Berlin, 1983.

(40) Sayers, D. E.; Bunker, B. A. In *X-Ray Absorption: Principles, Applications, Techniques of EXAFS, SEXAFS and XANES*; Koningsberger, D. C., Prins, R., Eds.; Wiley-Interscience: New York, 1988; Chapter 6.

(41) Cramer, S. P.; Hodgson, K. O.; Stiefel, E. I.; Newton, W. E. *J. Am. Chem. Soc.* **1978**, *100*, 2748.

(42) Suzuki, T. *J. Phys. Soc. Jpn.* **1960**, *15*, 2018.

(43) (a) Asplund, M.; Jagner, S.; Nilsson, M. *Acta Chem. Scand., Ser. A* **1983**, *37*, 57. (b) Asplund, M.; Jagner, S.; Nilsson, M. *Acta Chem. Scand., Ser. A* **1982**, *36*, 751.

(44) Lawn, B. R. *Acta Crystallogr.* **1964**, *17*, 1341.

(45) Otte, H. M. *J. Appl. Phys.* **1961**, *32*, 1536.

(46) (a) Johansson, G. *Acta Chem. Scand., Ser. A* **1971**, *25*, 2587. (b) Johansson, G. *Acta Chem. Scand.* **1966**, *20*, 553.

(47) Sandström, M.; Persson, I.; Ahrlund, S. *Acta Chem. Scand., Ser. A* **1978**, *32*, 607.

(48) Persson, I.; Sandström, M.; Goggin, P. L.; Mosset, A. *J. Chem. Soc., Dalton Trans.* **1987**, 1597.

(49) Johansson, G.; Sandström, M. *Chem. Scr.* **1973**, *4*, 195.

(50) Molund, M.; Persson, I. *Chem. Scr.* **1985**, *25*, 197.

(51) Magini, M.; Licheri, G.; Paschina, G.; Piccaluga, G.; Pinna, G. *X-Ray Diffraction of Ions in Aqueous Solutions: Hydration and Complex Formation*; CRC Press: Boca Raton, FL, 1988; Chapter 2.

(52) Sandström, M. *Acta Chem. Scand., Ser. A* **1978**, *32*, 627.

Table II. EXAFS Results: Interatomic Distances, $d/\text{\AA}$, Relative Square Deviations, $\sigma^2/\text{\AA}^2$ ($=1/4^2$), and Average Number of Distances, n , per Copper Atom in the Solution^b

solution	complex	dist	d	$10^{-3}\sigma^2$	n	F	P
50 mM Cu/Cl(MeCN)	CuCl ₂ ⁻	Cu-Cl	2.10 (2)	2.7	2.0	0.43	X
	CuCl ₂ ⁻	Cu-Cl	2.10 (2)	4.2	2.0		E
1 M Cu/Cl(Me ₂ SO)	CuCl ₂ ⁻	Cu-Cl	2.11 (2)	2.9	2.0	0.19	X
	CuCl ₂ ⁻	Cu-Cl	2.10 (2)	4.5	2.0		E
0.1 M Cu/Cl(py)	CuCl ₂ ⁻	Cu-Cl	2.12 (4)	12	2.0		E
0.2 M Cu/Cl(H ₂ O)	CuCl ₃ ²⁻	Cu-Cl	2.20 (2)	7.1	2.4	0.59	X
	CuCl ₂ ⁻	Cu-Cl	2.11	2.5	0.4	0.59	X
	CuCl ₃ ²⁻	Cu-Cl	2.21 (3)	9.5	3.0		E
88 mM Cu/Br(MeCN)	CuBr ₂ ⁻	Cu-Br	2.21 (2)	1.1	1.6	0.74	X
	[CuBr(MeCN) ₃]	Cu-Br	2.35 (5)	0.0	0.2	0.74	X
	[CuBr(MeCN) ₃]	Cu-N	2.01 (5)	0.0	0.6	0.74	X
	CuBr ₂ ⁻	Cu-Br	2.24 (3)	1.7	$\frac{1}{2} \times \mathbf{2.0}$	0.36	X
1.5 M Cu/Br(Me ₂ SO)	Cu ₂ Br ₄ ²⁻	Cu-Br	2.34 (4)	14	$\frac{1}{2} \times \mathbf{3.0}$	0.36	X
	Cu ₂ Br ₄ ²⁻	Cu-Cu	2.72 (8)	12	$\frac{1}{2} \times \mathbf{1.0}$	0.36	X
	CuBr ₂ ⁻	Cu-Br	2.25 (3)	5.5	$\frac{1}{2} \times \mathbf{2.0}$		E
	Cu ₂ Br ₄ ²⁻	Cu-Br	2.38 (4)	11	$\frac{1}{2} \times \mathbf{3.0}$		E
	[CuBr(py) ₃]	Cu-Br	2.42 (3)	12	1.0	0.21	X
0.4 M CuBr(py)	[CuBr(py) ₃]	Cu-N	2.04 (4)	7.6	3.0	0.21	X
	[CuBr(py) ₃]	Cu-Br	2.39 (3)	16	1.0		E
	[CuBr(py) ₃]	Cu-N	2.08 (3)	15	3.0		E
	Cu ₂ I ₄ ²⁻	Cu-I	2.59 (3)	17	3.0	0.18	X
1 M Cu/I(MeCN)	Cu ₂ I ₄ ²⁻	Cu-Cu	2.73 (8)	4.2	1.0	0.18	X
	Cu ₂ I ₄ ²⁻	Cu-I	2.54 (3)	5.5	3.0	0.33	X
1.5 M Cu/I(Me ₂ SO)	Cu ₂ I ₄ ²⁻	Cu-Cu	2.77 (8)	1.0	1.0	0.33	X

^aThe Debye-Waller factor is in the XFPKAG program a relative value: $\sigma^2 = \sigma_{\text{sample}}^2 - \sigma_{\text{ref}}^2$, where σ_{ref}^2 is obtained from the model compound. In the EXCURVE program σ^2 is an absolute value (the backscattering amplitude is obtained theoretically). The estimated error in σ^2 is ca. $1 \times 10^{-3} \text{\AA}^2$. ^bBoldfaced parameters have been held constant in the least-squares refinements. The goodness of fit is $F = \{\sum [k^3(\chi_{\text{obs}} - \chi_{\text{calc}})]^2/N\}^{1/2}$, where N is the number of data points. P denotes the program package used: X = XFPKAG and E = EXBACK + EXCURVE. The estimated error of the distances is given in parentheses.

formed in iodocuprate(I) solutions. The solids were examined in a rotating cell and generally showed better stability with the 647.1-nm laser line.

Results and Discussion

EXAFS of Chlorocuprate(I) Solutions. Available equilibrium constants⁸ show that the dominating chlorocuprate(I) complex should be CuCl₂⁻ at a large excess of chloride ions in dilute acetonitrile, dimethyl sulfoxide, and pyridine solutions. The EXAFS spectra of the 50 mM Cu/Cl(MeCN) and 1 M Cu/Cl(Me₂SO) solutions can be explained with a single shell of back-scattering chlorine atoms around copper (Figure 1a,b). Satisfactory least-squares curve fits of the unfiltered EXAFS data are obtained with two chlorine atoms at 2.10–2.11 Å (Table II), and the curve-fitting was not improved by the introduction of further backscatters.

For 13 well-determined ($\sigma < 0.005 \text{\AA}$) nearly linear CuCl₂⁻ complexes in crystal structures, the Cu-Cl distances are found in the range 2.07–2.12 Å with the mean value 2.09 Å.¹¹ For trigonal coordination, a mean Cu-Cl bond length of 2.22 Å is found in a discrete almost planar CuCl₃²⁻ complex,⁹ 2.27 Å is found for weak bridging interactions,⁵⁴ and 2.24 Å is found for a dimeric Cu₂Cl₄²⁻ complex with an asymmetric double bridge.⁵⁵ Mean values of Cu-Cl distances in some representative compounds with approximately tetrahedral four-coordination are 2.36,⁵⁶ 2.40,^{57,58} 2.41, and 2.42 Å.⁹ A large spread in the distances often occurs due to the difference in Cu-Cl distances between the terminal Cl atoms and those in the asymmetric bridges, but the mean values remain fairly constant; see also Table 8 of ref 21. Thus, the short Cu-Cl distance found for these chlorocuprate(I) solutions is a strong indication of a linear CuCl₂⁻ complex.

For the 0.1 M Cu/Cl(py) solution, the experimental data and the fit are less good, and a mean Cu-Cl distance of about 2.12 Å was obtained from the curve fit (Table II). However, the

equilibrium constants indicate that, despite the large Cl⁻ excess, about 25% of the copper(I) is present as the solvated CuCl complex,⁶ with a Cu-Cl distance expected to be somewhat longer than in the CuCl₂⁻ complex (see the discussion on the CuBr complex below). This would explain the larger uncertainty in the mean Cu-Cl distance, although it was not possible to analyze the data by using two slightly different Cu-Cl distances.

In the aqueous 0.2 M Cu/Cl(H₂O) solution, the CuCl₃²⁻ species should be dominating and about 20% of the copper(I) should be present in CuCl₂⁻ complexes according to the equilibrium constants.² The curve fit of the EXAFS data gave an acceptable result for three chloride ions around the copper atom with a mean Cu-Cl distance of about 2.21 Å (Table II), close to the crystal structure value of ca. 2.22 Å for a discrete mononuclear CuCl₃²⁻ complex.⁹ We could not resolve two shells in the EXAFS data, although the fit improved noticeably after introducing the expected contribution from a linear CuCl₂⁻ complex in the model.

EXAFS of Dibromocuprate(I) and Copper(I) Bromide. The stability constants indicate a dominating CuBr₂⁻ complex with about 20% monomeric CuBr present in the 88 mM Cu/Br(MeCN) solution.⁴ A satisfactory curve fit of the EXAFS data was obtained for a major species with two bromide ions 2.21 (2) Å from the copper atom and with Cu-Br and Cu-N distances corresponding to expected values for a minor amount of a [CuBr(MeCN)₃] complex; see Table II. The short Cu-Br distance, within the range 2.21–2.23 Å for linear [CuBr₂]⁻ ions in solid compounds,^{9–11} indicates a similar structure in solution.

A Fourier transform of the EXAFS of the 0.4 M CuBr(py) solution showed a main peak with at least two components. The analysis of the EXAFS data gave a satisfactory curve fit (Figure 1c), with three nitrogen atoms at 2.06 (4) Å and one bromine atom at 2.41 (3) Å. This is in good agreement with some Cu(I)-N(py) distances previously found in tetrahedral coordination, e.g. 2.046 (4) at 260 K,⁵⁹ 2.05 (2) Å (room temperature)⁶⁰ in the [Cu(py)₄]⁺ complex in the solid state, and 2.06 (1) Å in pyridine solution,³⁶ although shorter distances occur in the polymeric CuX-py compounds, 1.99, 2.00, and 2.04 Å for X = Cl, Br, and I, respec-

(53) Nakamoto, K. *Infrared and Raman Spectra of Inorganic and Coordination Compounds*, 4th ed.; Wiley: New York, 1986.

(54) Banci, L.; Bencini, A.; Dei, A.; Gatteschi, D. *Inorg. Chim. Acta* **1984**, *84*, L11.

(55) Scott, B.; Willett, R. *Inorg. Chem.* **1991**, *30*, 110.

(56) Baglio, J. A.; Vaughan, P. A. *J. Inorg. Nucl. Chem.* **1970**, *32*, 803.

(57) Brink, C.; van Arkel, A. E. *Acta Crystallogr.* **1952**, *5*, 506.

(58) Simonsen, O.; Toftlund, H. *Acta Crystallogr.* **1987**, *C43*, 831.

(59) Nilsson, K.; Oskarsson, Å. *Acta Chem. Scand., Ser. A* **1982**, *36*, 605.

(60) Lewin, A. H.; Michl, R. J.; Ganis, P.; Lepore, U.; Avitabile, G. *J. Chem. Soc., Chem. Commun.* **1971**, 1400.

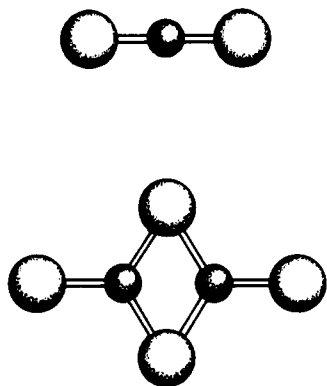


Figure 3. Structures of the CuX_2^- and $\text{Cu}_2\text{X}_4^{2-}$ complexes.

tively,^{25,29,30} with copper(I) in a tetrahedral environment of one pyridine molecule and three bridging halide atoms. The EXAFS value of the Cu–Br distance, 2.41 Å, is slightly longer than in trigonal CuBr_2^{2-} complexes, 2.365 (3) and 2.355 Å,^{9,16} but shorter than the mean values obtained in compounds with copper(I) coordinating four bromide ions, 2.52 and 2.503 (4) Å.^{10,56} Significantly shorter bond distances occur for two-coordinated complexes, e.g. in the discrete monomeric complex LCuBr (L = 2,2,6,6-tetramethylpiperidine) with Cu–N = 1.931 (9), 1.935 (7) Å and Cu–Br = 2.216 (2), 2.202 (2) Å.²⁴ The distance correlations imply that in the 0.4 M $\text{CuBr}(\text{py})$ solution the dominating complex is $[\text{CuBr}(\text{py})_3]$.

The Fourier transform of the EXAFS of the concentrated 1.5 M $\text{Cu}/\text{Br}(\text{Me}_2\text{SO})$ solution is dominated by the Cu–Br shell. The most satisfactory fit of the EXAFS data (Figure 1d) was obtained for a model corresponding to about equal concentrations of the CuBr_2^- and $\text{Cu}_2\text{Br}_4^{2-}$ complexes (Figure 3). A Cu–Br distance of 2.24 (3) Å was obtained for the CuBr_2^- complex and an average Cu–Br distance of 2.36 (4) Å for the dimeric $\text{Cu}_2\text{Br}_4^{2-}$ complex, to be compared with the mean value of 2.40 Å from six $\text{Cu}_2\text{Br}_4^{2-}$ complexes in crystal structures.^{11,22}

EXAFS of Iodocuprate(I) Solutions. The Fourier transforms of the EXAFS data from the concentrated iodocuprate(I) solutions in acetonitrile and dimethyl sulfoxide are strongly dominated by a Cu–I interaction at about 2.57 Å, consistent with trigonal Cu–I coordination as in a $\text{Cu}_2\text{I}_4^{2-}$ complex. From eight well-determined crystal structures with $\text{Cu}_2\text{I}_4^{2-}$ complexes, a mean Cu–I distance of 2.55 Å is obtained,^{18,23} which is much shorter than the mean Cu–I distances 2.68–2.69 Å in dimeric $\text{Cu}_2\text{I}_6^{4-}$ or $\text{Cu}_2\text{I}_5^{3-}$ complexes with copper(I) in approximately tetrahedral coordination.^{18,20} The curve fits of the EXAFS data (Figure 1e,f) are markedly improved by the introduction of a Cu–Cu distance of about 2.7 Å, as expected for a $\text{Cu}_2\text{I}_4^{2-}$ complex (Figure 3).

For the more dilute iodocuprate(I) solutions studied, the poor quality of the EXAFS data prevented detailed analyses, but the edge structure in the XANES region gave information on the type of coordination in the dominating copper(I) complex; see below.

Absorption Edges. A preedge transition occurs at about 8983–4 eV for all the copper(I) complexes studied (Figure 4) and has been assigned as the dipole-allowed Cu 1s → 4p transition.³⁷ This absorption line is very intense for copper(I) in linear two-coordination,³⁷ although its relative magnitude seems to decrease somewhat with increasing size and “softness” of the coordinated halide ion. The linear CuCl_2^- complex in the solid $[(\text{C}_4\text{H}_9)_4\text{N}]\text{CuCl}_2$ and in the 50 mM $\text{Cu}/\text{Cl}(\text{MeCN})$ and 1 M $\text{Cu}/\text{Cl}(\text{Me}_2\text{SO})$ solutions (Figure 4A–C) gives rise to virtually identical spectra in the edge region. The similar features of the spectra of the solid $[(\text{C}_4\text{H}_9)_4\text{N}]\text{CuBr}_2$ and the 88 mM $\text{Cu}/\text{Br}(\text{MeCN})$ and 1.5 M $\text{Cu}/\text{Br}(\text{Me}_2\text{SO})$ solutions (Figure 4D–F) show that two-coordinated CuBr_2^- complexes are present in the bromocuprate(I) solutions. Also, the dilute 50 and 60 mM iodocuprate(I) solutions in acetonitrile and pyridine (Figure 4G,H) evidently contain some amount of two-coordinated CuI_2^- complexes.

For copper(I) in trigonal three-coordination, the 8983-eV line is reduced to a shoulder and an additional absorption feature at

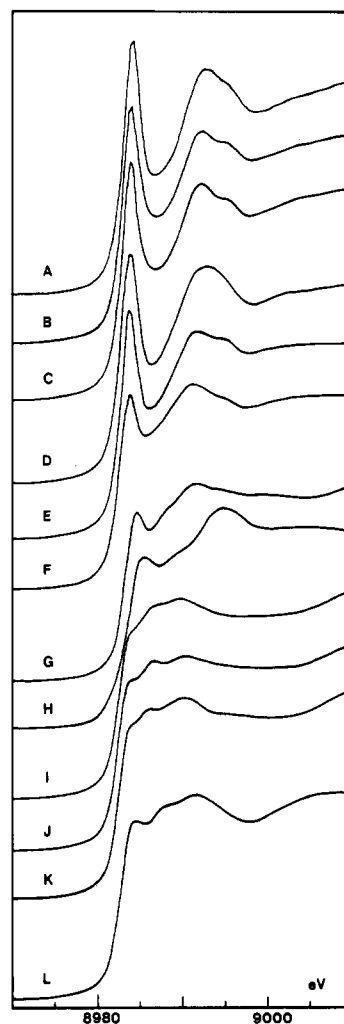


Figure 4. Absorption edge spectra: (A) $[(\text{C}_4\text{H}_9)_4\text{N}][\text{CuCl}_2](\text{s})$; (B) 50 mM $\text{Cu}/\text{Cl}(\text{MeCN})$; (C) 1 M $\text{Cu}/\text{Cl}(\text{Me}_2\text{SO})$; (D) $[(\text{C}_4\text{H}_9)_4\text{N}][\text{CuBr}_2](\text{s})$; (E) 88 mM $\text{Cu}/\text{Br}(\text{MeCN})$; (F) 1.5 M $\text{Cu}/\text{Br}(\text{Me}_2\text{SO})$; (G) 50 mM $\text{Cu}/\text{I}(\text{MeCN})$; (H) 60 mM $\text{CuI} + 0.7 \text{ M NH}_4\text{I}$ in pyridine; (I) 1.5 M $\text{Cu}/\text{I}(\text{Me}_2\text{SO})$; (J) 1 M $\text{Cu}/\text{I}(\text{MeCN})$; (K) $[(\text{C}_4\text{H}_9)_4\text{N}]_2[\text{Cu}_2\text{I}_4](\text{s})$; (L) 0.2 M $\text{Cu}/\text{Cl}(\text{H}_2\text{O})$.

about 8986 eV becomes visible, because of the splitting of the p-orbital energies.³⁷ Spectra of this type, with very similar appearance, are obtained for samples where $\text{Cu}_2\text{I}_4^{2-}$ complexes dominate, i.e. the solid compound $[(\text{C}_4\text{H}_9)_4\text{N}]_2[\text{Cu}_2\text{I}_4]$ (Figure 4K) and the concentrated dimethyl sulfoxide and acetonitrile solutions of Figure 4I,J. The edge structure of 0.2 M $\text{Cu}/\text{Cl}(\text{H}_2\text{O})$ (Figure 4L) is consistent with a dominant trigonal CuCl_2^- complex in aqueous solution, while the edge of the 1.5 M $\text{Cu}/\text{Br}(\text{Me}_2\text{SO})$ solution (Figure 4F) has features of both linear and trigonal structure types.

LAXS Studies of $\text{Cu}_2\text{X}_4^{2-}$ Complexes. The major peaks in the RDF's (Figure 2) are found at 2.6 and 4.4 Å for the concentrated iodocuprate(I) solutions in dimethyl sulfoxide and acetonitrile and at 2.4 and 4.1 Å for the bromocuprate(I) complexes in dimethyl sulfoxide solution. The broad peaks below 2 Å correspond to intramolecular distances within the solvent molecules.⁵²

For a planar $\text{Cu}_2\text{I}_4^{2-}$ complex with a structure according to Figure 3, peaks with positions and sizes in good agreement with those in the experimental RDF's (Figure 2) can be calculated by a Fourier transformation of the $i_c(s)$ intensities from eq 1 with parameters according to Table III. The numbers of atom-pair interactions were held constant at the expected values for a dimer, 3 Cu–I and 2.5 I–I distances per copper atom in the complex, in the least-squares refinements of mean distances and temperature coefficients performed on the high-angle region of the reduced intensity curves. The Cu–Cu distance makes an insignificant contribution to the $i_c(s)$ values but was included with constant

Table III. Interatomic Distances, $d/\text{\AA}$, Temperature Factor Coefficients for the Distances, $l/\text{\AA}$, and Frequencies, n , of the Distances Relative to One Copper Atom for the $\text{Cu}_2\text{I}_4^{2-}$ Complexes in Acetonitrile and Dimethyl Sulfoxide and for CuBr_2^- and $\text{Cu}_2\text{Br}_4^{2-}$ in Dimethyl Sulfoxide from the LAXS Study^a

solution (s range)	complex	dist	d	l	n
1 M Cu/I(MeCN) (4–16 \AA^{-1})	$\text{Cu}_2\text{I}_4^{2-}$	Cu–I	2.574 (4)	0.12 (3)	3.0
		I–I	4.42 (1)	0.22 (6)	2.5
		Cu–Cu	2.68	0.10	0.5
1.5 M Cu/I(Me_2SO) (5–16.5 \AA^{-1})	$\text{Cu}_2\text{I}_4^{2-}$	Cu–I	2.579 (5)	0.14 (4)	3.0
		I–I	4.41 (1)	0.21 (6)	2.5
		Cu–Cu	2.68	0.12	0.5
1.5 M Cu/Br(Me_2SO) (5–16 \AA^{-1})	$\text{Cu}_2\text{Br}_4^{2-}$	Cu–Br	2.377 (4)	0.11 (4)	1.5
		Br–Br	4.02 (2)	0.24 (7)	2.5
	CuBr_2^-	Cu–Cu	2.68	0.12	0.5
		Cu–Br	2.24 (1)	0.06 (2)	1.0
		Br–Br	4.46 (2)	0.04 (6)	0.5

^aThe refined parameters are those with estimated standard deviations from the least-squares procedure given in parentheses.

estimated parameter values. The Cu–I distance obtained, 2.58 (1) \AA (Table III), is close to the expected mean Cu–I distance, 2.55 \AA , from $\text{Cu}_2\text{I}_4^{2-}$ complexes in crystal structures^{18,23} and to the EXAFS results (Table II).

For the 1.5 M Cu/Br(Me_2SO) solution, the peaks are smaller and broader than expected for a dominating $\text{Cu}_2\text{Br}_4^{2-}$ complex, and according to the Raman and EXAFS spectra (Figures 5 and 4F), some amount of CuBr_2^- is present. The best fit of the calculated model was obtained when equal concentrations of CuBr_2^- and $\text{Cu}_2\text{Br}_4^{2-}$ were assumed. The parameters obtained from the model refinements on the intensity data are given in Table III, and the corresponding peak shapes obtained by a Fourier transform are shown in Figure 2. The mean Cu–Br distance for the dimer, 2.38 (1) \AA , from the LAXS study of the 1.5 M Cu/Br(Me_2SO) solution is in acceptable agreement with the average EXAFS value, 2.36 (4) \AA , and crystal structure distances (see above). The remaining broad peaks around 5 \AA mainly originate from the pronounced solvent bulk structure, as was also found previously for neat dimethyl sulfoxide and in other dimethyl sulfoxide solutions.^{52,61} This makes detailed conclusions on the halide–halide interactions in the complexes difficult from the RDF's, especially for the bromocuprate(I) solution. However, the intramolecular halide–halide interactions will still contribute to the reduced intensity in the high-angle region of the model fitting, for which the more diffuse solvent–solvent contributions are negligible. This is evident in particular for the iodocuprate complexes, but also for the bromocuprate(I) solution, where the refinements of the main X–X interactions give results consistent with a dimeric $\text{Cu}_2\text{X}_4^{2-}$ complex.

The $\text{Cu}_2\text{X}_4^{2-}$ complexes in solids have shorter Cu–X bond lengths to terminal halide atoms than to bridging. The mean differences are 0.09 and 0.14 \AA for the Cu–I and Cu–Br bonds in 11 and 6 crystal structures, respectively.^{11,22} A similar difference probably persists also in solution. It is difficult, however, to resolve two distances of the same kind closer than about 0.2 \AA with LAXS or EXAFS methods, but a larger spread in the distance than caused by the thermal movements will broaden the corresponding peak in the RDF function and increase its thermal parameter value. This seems to be the case for the $\text{Cu}_2\text{X}_4^{2-}$ complexes in the dimethyl sulfoxide and acetonitrile solutions, with l parameters larger than expected, in particular for the mean Cu–I distances. The root-mean-square variation, $l = (2b)^{1/2}$, of a metal–halide distance in a HgX_3^- complex was previously found to be about 0.08 \AA ,^{52,62} compared to 0.12–0.14 \AA in $\text{Cu}_2\text{X}_4^{2-}$ in this study.

Vibrational Spectroscopic Studies. The vibrational frequencies obtained in this study for the CuX_2^- complexes in acetonitrile, dimethyl sulfoxide, and pyridine solutions and in the tetrabutylammonium salts are summarized in Table IV, together with previously reported values for solutions. Raman and IR spectra

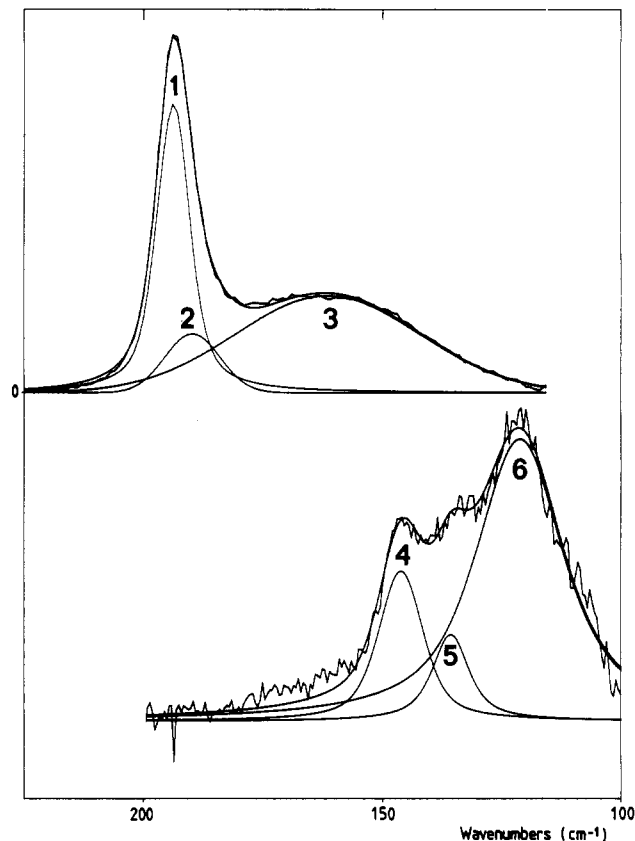


Figure 5. Raman spectra of 1.5 M Cu/Br(Me_2SO) and 1.5 M Cu/I(Me_2SO) after subtraction of NH_4Br and NH_4I solution spectra in dimethyl sulfoxide, respectively. The sharp bands at 194 and 146 cm^{-1} (nos. 1 and 4) correspond to the ν_1 symmetric stretching vibration transitions of the CuBr_2^- and CuI_2^- complexes, respectively, and the bands from the curve-fitting at about 190, 162 cm^{-1} and 136, 122 cm^{-1} (nos. 2, 3 and 5, 6) are from the $\text{Cu}_2\text{Br}_4^{2-}$ and $\text{Cu}_2\text{I}_4^{2-}$ complexes, respectively.

of the $[\text{K}(18\text{-crown-6})\text{CuI}_2]$ compound gave bands in good agreement with those found for the CuI_2^- complex in tri-*n*-butyl phosphate solution (Table IV).

For the CuX_2^- complexes no observations were made of coincident bands in Raman and IR spectra, which would have shown deviations from $D_{\infty h}$ symmetry. The stretching Cu–X vibrational frequencies observed in solution are close to the values found in the solid state (Table IV). This is a strong indication that no solvent molecules are coordinated in the inner coordination sphere of copper(I) in the solvents studied, in contrast to what was found previously for the HgX_2 complexes, for which large changes in the Hg–X stretching vibration frequencies occurred.^{32,33} The symmetric stretching vibration transitions $\nu_1(\text{XHgX})$ of the solvated HgX_2 complexes in dimethyl sulfoxide solution occur at the wavenumbers 303, 195, and 145 cm^{-1} for X = Cl, Br, and I, respectively.^{32,33} The corresponding vibrations of the linear CuCl_2^- and CuBr_2^- complexes in the solid state, 302 and 194 cm^{-1} , respectively, are very close to those observed for the CuCl_2^- and CuBr_2^- complexes in dimethyl sulfoxide solutions, 301 and 193 cm^{-1} . (Although the mercury(II) complexes show a much larger shift from gas-phase values upon solvation in dimethyl sulfoxide, they are still only slightly bent, with X–Hg–X angles of about 165°; cf. ref 32, Table III.) The stretching force constants of the CuX_2^- and HgX_2 complexes have previously been found to decrease in the same order from X = Cl to I.¹⁷ On the basis of the above comparisons, the Raman band at 147 cm^{-1} in the $[\text{K}(18\text{-crown-6})\text{CuI}_2]$ compound and the 146- cm^{-1} band of the concentrated iodocuprate(I)/dimethyl sulfoxide solutions have been assigned to the $\nu_1(\text{ICuI})$ symmetric stretching vibration of the CuI_2^- ion (Table IV).

The Raman spectra of the concentrated bromo- and iodocuprate(I)/dimethyl sulfoxide solutions are shown in Figure 5, and the Raman and IR wavenumbers in Table IV. The sharp

(61) Ahrlund, S.; Hansson, E.; Iverfeldt, Å.; Persson, I. *Acta Chem. Scand., Ser. A* 1981, 35, 275.

(62) Gaizer, F.; Johansson, G. *Acta Chem. Scand., Ser. A* 1968, 22, 3013.

Table IV. Vibration Transition Wavenumbers, $\bar{\nu}/\text{cm}^{-1}$, of Halocuprate(I) Complexes in the Solid State and in Solution^a

sample	IR	Raman
Solids		
[(C ₄ H ₉) ₄ N][CuCl ₂]	407 s (ν_3), 108 m (ν_2)	302 m (ν_1)
[(C ₄ H ₉) ₄ N][CuBr ₂]	326 s (ν_3), 81 m (ν_2)	194 m (ν_1)
[K(18-crown-6)][CuI ₂]	281 m (ν_3)	147 m (ν_1)
[(C ₄ H ₉) ₄ N] ₂ [Cu ₂ I ₄]	172 m, 154 m (ν_2) 136 vw, 93 w, 70 m, 64 w	122 m, 66 w
[(C ₂ H ₅) ₄ N] ₂ [Cu ₂ I ₄] ^b	172	204, 143, 126
[(C ₂ H ₅) ₄ N] ₂ [Cu ₂ Br ₄] ^b	218	235, 170, 160
[Cu(py) ₄]ClO ₄	~178 w, 162 m	177 m, ~160 w
Solutions		
0.5 M Cu/Cl(MeCN)	409 s (ν_3)	305 m (ν_1)
1 M Cu/Cl(Me ₂ SO)	410 m (ν_3), ~115 w (ν_2)	301 m (ν_1)
0.1 M Cu/Cl(py)	~114 w (ν_2)	
0.15 M CuCl ₂ ⁻ in TBP ^c	405 (ν_3), 109 (ν_2)	300 (ν_1)
CuCl ₂ ⁻ in ether extract ^d		296 (ν_1)
[(C ₂ H ₅) ₃ NH] ⁺ [CuCl ₂] ⁻ (I) ^e		302 (ν_1), 270–310
88 mM Cu/Br(MeCN)	326 (ν_3)	
1 M Cu/Br(MeCN)	326 w (ν_3)	192 m (ν_1)
1.5 M Cu/Br(Me ₂ SO) ^f		194 m (ν_1), ~190 vw, ~162 m
0.23 M CuBr ₂ ⁻ in TBP ^c	322 (ν_3), 81 (ν_2)	193 (ν_1)
0.08 M CuBr ₂ ⁻ in ethanol ^g	323	
CuBr ₂ ⁻ in nitromethane ^h	321	
CuBr ₂ ⁻ in ether extract ^d		190
0.4 M CuBr(py)	171 w, 145 w	155 vw
1 M Cu/I(MeCN)	200 m	~122 vw
1.5 M Cu/I(Me ₂ SO) ^f	155 w	146 m (ν_1), ~136 vw, ~122 m
0.35 M CuI ₂ ⁻ in TBP ^c	279 (ν_3), 65 (ν_2)	148 (ν_1)

^a Strong, medium, weak, and very weak bands are denoted s, m, w, and vw, respectively. For the linear CuX₂⁻ complexes assignments are given as $\nu_1(\Sigma_g^+$, symmetric stretch), $\nu_2(\Pi_u^+$, asymmetric stretch), and $\nu_3(\Sigma_u^+$ bend). Estimated error limits are within $\pm 1 \text{ cm}^{-1}$ if not otherwise indicated. ^b Reference 17. ^c Reference 31; TBP = tri-*n*-butyl phosphite. ^d Reference 64. ^e Reference 65. ^f Figure 5. ^g Reference 10. ^h Reference 13.

well-defined bands of the linear CuX₂⁻ complexes are visible at much lower concentrations than those of the dimeric Cu₂X₄²⁻ complexes. For the 1.5 M Cu/I(Me₂SO) solution, in which the amount of copper(I) present in a CuI₂⁻ complex is estimated from the LAXS results to be less than 5%, there is still a clearly visible band at 146 cm⁻¹ in the Raman spectrum (Figure 5). For the 1 M Cu/I(MeCN) solution, however, only the broad band at ~122 cm⁻¹ corresponding to Cu₂I₄²⁻ could be seen, which shows that the CuI₂⁻ concentration is low. The CuBr₂⁻ complex in the 1.5 M Cu/Br(Me₂SO) solution gives a strong Raman band at 194 cm⁻¹, while the broad band at about 162 cm⁻¹ from the Cu₂Br₄²⁻ complex is less obvious, despite the high concentration of this complex (Figure 5).

Weak intensities and broad bands, especially in the Raman spectra, are obtained from the pyridine and aqueous solutions, features which seem to be rather general for nonlinear copper(I) compounds,^{15,17} and possibly are connected to a relatively low degree of covalency in the bonds.⁶³ For the [Cu(py)₄]ClO₄ compound the bands at 177 and 162 cm⁻¹ probably correspond to the symmetric and asymmetric Cu–N stretching modes, respectively, of the tetrahedrally coordinated [Cu(py)₄]⁺ ion.⁵⁹ However, no unambiguous assignment of the bands observed for the 0.4 M solution of CuBr in pyridine (Table IV) could be made.

The ν_3 band in the IR spectrum of the CuCl₂⁻ complex dominating in the 0.1 M Cu/Cl(py) solution is obscured by a solvent

band, although a weak ν_2 band is visible at 114 cm⁻¹. However, the 405-cm⁻¹ out-of-plane ring deformation band of the free pyridine is partly shifted and gives a new band at 420 cm⁻¹, a feature observed upon complex formation.⁵³ This supports the presence of some amount of a [CuCl(py)₃] complex in this solution, as indicated from the EXAFS results.

Concluding Remarks. The copper(I) cation has previously been found to be tetrahedrally solvated in the solvents used in this study.^{36,59} For CuBr in pyridine solution, the distances Cu–N = 2.06 (3) Å and Cu–Br = 2.41 (3) Å are found, consistent with a tetrahedral [CuBr(py)₃] complex. The comparisons of distances and vibrational frequencies between solid state and solution show that the dihalocuprate(I) complexes retain a linear structure in the solvents studied. No coordination of solvent molecules to the copper(I) ion is found for the CuX₂⁻ complexes in any of the solvents in Table IV. This implies that the tetrahedral configuration of copper(I) remains when the first copper(I) halide complex is formed and that a coordination change with an extensive desolvation takes place at the formation of the second complex, consistent with the thermodynamics of the complex formation previously reported.⁶⁶

The tendency of the dihalocuprate(I) complexes to dimerize at high total concentrations increases markedly with increasing size of the halide. From the LAXS and EXAFS results, it is possible to estimate the range of the equilibrium constant for the dimerization, $K = c_{\text{Cu}_2\text{X}_4^{2-}}/c_{\text{CuX}_2^-}^2$. The estimated K values are <0.2, ≈2, and >100 mol⁻¹ dm³ for the concentrated chloro, bromo, and iodo solutions in dimethyl sulfoxide, respectively, and >200 mol⁻¹ dm³ for the 1 M Cu/I(MeCN) solution. The coordination around copper(I) changes from linear to trigonal upon dimerization, and a double halide bridge is formed, as in the dimers found in crystal structures.^{9–11,21,22}

The linear CuX₂⁻ complexes are not as easily perturbed in solution as the HgX₂ complexes, which can adopt pseudotetrahedral configurations with the X–Hg–X angle varying between 180 and 100°, depending on the solvating ability of the solvent.^{32,33} When unperturbed or sterically unhindered, the ligands around copper(I) seem to adopt only the electrostatically favored configurations linear, trigonal, and tetrahedral, while mercury(II) has a much more flexible coordination geometry. The larger tendency toward linearity for copper(I) than for mercury(II) complexes has been suggested to be a result of the smaller d–s excitation energy and increased configurational mixing (second-order Jahn–Teller effects) of the corresponding states.^{17,67} However, the negative charge of the CuX₂⁻ complexes is probably more important in inhibiting the distortion of the linear coordination by solvation than d–s mixing in the bonding Cu(I)–X orbitals, as indicated by the comparison with HgX₂.

Acknowledgment. The support from the Swedish Natural Science Research Council, Knut and Alice Wallenberg Foundation, and Carl Tryggers Stiftelse is gratefully acknowledged. We thank the SERC for an allocation of the EXAFS service. We are grateful to Prof. R. A. Scott, University of Georgia, for providing us with the XFPACK program package and to Dr. Peter L. Goggin for the use of the Nicolet FT-IR spectrometer at the University of Bristol.

Registry No. CuCl₂⁻, 15697-16-2; CuBr₂⁻, 18007-70-0; CuI₂⁻, 30291-68-0; CuBr₄²⁻, 14337-09-8; CuI₄²⁻, 63796-60-1; CH₃CN, 75-05-8; [CuBr(py)₃], 36545-29-6; [Cu(py)₄]ClO₄, 21465-66-7; pyridine, 110-86-1.

Supplementary Material Available: Figures showing model fitting of the LAXS data with experimental and calculated $si(s)$ values, Fourier transforms of the raw copper EXAFS data, with Gaussian windows for the filtering of the back-transforms used for curvefits, the transforms of the fitted theoretical EXAFS functions, and plots of unfiltered EXAFS data of samples not included in Figure 1 (25 pages). Ordering information is given on any current masthead page.

(63) Bowmaker, G. A.; Dyason, J. C.; Healy, P. C.; Engelhardt, L. M.; Pakawatchai, C.; White, A. H. *J. Chem. Soc., Dalton Trans.* **1987**, 1089.

(64) Creighton, J. A.; Lippincott, E. R. *J. Chem. Soc.* **1963**, 5134.

(65) Porterfield, W. W.; Yoke, J. T. In *Inorganic Compounds with Unusual Properties*; King, B., Ed.; Advances in Chemistry 150; American Chemical Society: Washington, DC, 1976; Chapter 10, p 104.

(66) Ahrlund, S.; Ishiguro, S.-I. *Inorg. Chim. Acta* **1988**, *142*, 277.

(67) Pearson, R. G. *Symmetry Rules for Chemical Reactions*; Wiley: New York, 1976; Chapters 1 and 3.